IET Research Journals

Improved version of the VPPC 2018 Paper for the IET Electrical Systems in Transportation

ISSN 1751-8644
doi: 0000000000
www.ietdl.org

Off-board and On-board Energy storage Vs. Reversible Substations in DC Railway Traction Systems

Pablo Arboleya[1*], *Bassam Mohamed*[1], *Islam El-Sayed*[1]

[1] *LEMUR Research Group, Electrical Engineering Department, University of Oviedo, Campus of Gijón, Building 4, Office 4.02.09, Gijón, Spain*
* *E-mail: arboleyapablo@uniovi.es*

Abstract: The present paper describes and analyzes a set of quasi-static railway power systems models and simulations considering on-board and off-board energy storage systems but also reversible and non-reversible substations and regenerative braking trains. The advantages and drawbacks of each technology are discussed. Then, several case studies considering different technological combinations are introduced and simulated, while the attained results are compared and analyzed. In this regard, to cover all the casuistic, two simple explanatory cases are firstly exposed to then examine eight realistic scenarios that are simulated for a long time interval and explained considering also aggregated results.

1 Introduction

Modern railways feeding systems, similarly to other conventional power delivery infrastructures, are rapidly evolving including new technologies and devices [1]. In most of the cases, this evolution relates with the inclusion of modern power electronics and energy storage devices into the networks [2, 3] or in vehicles [4]. Nonetheless, some researchers are also working on new techniques for connecting renewable energy generation with locomotive traction purposes [5] or applying the smart grid paradigm to the railway systems [6]. Traditionally, railway power systems designers have been very conservative and reluctant to changes, a proof of that is the fact that most of the feeding substations in DC railways systems are based on non-controllable diode rectifiers [7]. Nevertheless, the change towards new technologies is a fact in these days [2]. Even though most of the trains are equipped with regenerative braking systems [8, 9], the use of this technology is not enough for increasing the overall efficiency of the system if it is not coordinated with other technologies or operation philosophies. Hence, the proper coordination of the trains schedule for creating more efficient traffic scenarios is an option in which many researchers are working [10, 11]. To take advantage of this last strategy while using regenerative braking trains, it is also highly important to consider the limited network receptivity [12]. This receptivity is even lower when trains are not coordinated and technologies like reversible substations and on-board/off-board energy storage are not installed into the traction system [13, 14].

The use of the aforementioned technologies in a coordinated manner can lead to a significant increase in the overall efficiency of the system and its controllability [13, 15, 16]. For instance, in [17] the authors present a study held for the 6.6km Thessaloniki metro line in which they expose the power quality benefits as well as the advantages of installing reversible substations or wayside accumulation systems considering a headway between trains of 300s. In both cases the system is modelled as an optimisation problem considering the implementation feasibility of a real time centralised controller. In this regard, the development of computer tools for carrying out the system analysis and achieve the optimum technological mix and its coordination is mandatory [18]. Nowadays, there are many research lines chasing this objective. For instance, a static simulator to analyse the impact of the wayside energy storage along the network is proposed in [19]. There, the authors propose a model to study a specific scenario and evaluate the recovering surplus of regeneration braking energy, voltage stabilization and reduction of peak power demand obtained with this technology. In [20], a simulation is carried out with Modelica software to model a specific line in Bergamo (North of Italy). This line is a 12km tramline with 10 substations containing up to 10 trains. Again, non-reversible substations and wayside energy storage are considered. However, the authors do not provide details of the train model and neither specify if a complex control for modeling the interaction between the train and the system was considered or not. In [21], the impact of installing reversible substations and accumulation devices over the efficiency of the system is determined. For that purpose, a traffic simulation scenario with a power flow solver are integrated. In [16], a formulation is proposed to evaluate the efficiency increment when adding energy storage at substation level. The AC network analysis is included performing a hybrid AC/DC power flow. Nevertheless, the non-reversibility of the diode based substations and the train protection curves (overcurrent and overvoltage) are not considered. For this case, the non-reversibility behaviour is not necessary to be modeled as the reverse power flows are absorbed by the substation storage devices. Within this approach, the train model is embedded in the power flow while the vehicle and power system are solved in a coupled way. This methodology is applied to a 100km-3kV line between Firenze and Livorno. The work presented in [22] propose the use of multiport converters in order to add energy storage at substation level in a 3kV DC line. Real data from a 24km Italian regional line from Saronno to Como Lake is employed. The multiport device is connected in series with the conventional diode rectifier to allow power flow control from the DC to the AC system and the energy storage device. In [11] a hybrid centralised-decentralised approach for improving the energy management of all devices present in the DC railway system is exhibited. The centralised system is run in a day-ahead scenario while the decentralised energy management operates in intervals of a few minutes ahead. This approach considers also the trains speed profiles to then suggest some changes on them. Both problems, centralised and decentralised are stated as an optimization problem.

From another perspective, some researchers propose the use of highly complex and accurate dynamical models of the trains and the network [14, 23, 24]. Nonetheless, the computational burden of these models is too high in some cases and their application to extensive traction systems with a large number of trains is intricate. In [23], a very detailed model of a subway is presented using the well known Energetic Macroscopic Representation (EMR). This model is applied for simulation on a 15km single line and single train scenario. Experimental results are validated with real measurements. A similar approach is presented in [24] and [25]. Another example of dynamic simulation can be found in [26]. In

this work, the train and the non reversible substation are modeled together in MATLAB/Simulink considering different energy storage technologies and controls. This approach is intended to study the impact of energy storage systems over the network under a multi-train scenario. The tests are conducted for a line 7 section of the New York City Transit System including 3 substations and 4 passenger stations. Several speed profiles are considered but only for one train. The results are validated with real measurements samples at 5kHz but no information is provided about the simulation sampling period or the influence in the number of trains and substations. In [27], a small-signal model for dynamic analysis of the railway system is exposed considering the trains and the substations but also photovoltaic generation in the DC traction system. Modelling and control of VSC-based reversible substations, PV plants and trains is exhibited. A similar approach can be observed in [28, 29], but in this case the authors use a commercial software package (RAILSIM) for the railway simulation and a mixed integer linear programming (MILP) algorithm in GAMS software package to carry out the optimization.

In other cases, the authors present quasi-static models where every time instant is solved independently assuming a steady state condition; such is the case of [12, 13]. The quasi-static philosophy is simpler and more flexible as it allows the simulation of very large networks with a great number of trains. Within this approach, still enough accuracy is attained for planning and operation purposes. In most of the cases the train and the network models are solved in a decoupled way while the control of the train overcurrent and overvoltage is implemented to take into account the limited receptivity of the network. When the decoupled tactic is considered, the power reference and position data of the train are usually obtained from a different software suite like the one presented in [30]. There the authors propound a driving mode optimisation to attain the best trajectory. The results can later be used to train the drivers or implement automatic driving systems by means of the infrastructure simulation software. In this specific case, the system is tested in a 13.77km path with 15 stations connecting Edimburgh with its Airport for a train with a maximum traction power of 907kW and a maximum speed of 70km/h. In [31], the authors propose a pseudo-static modelling of a reversible substation to analyse the effect of the different regulation parameters over the burned and regenerated power among others. To do so, the power flow simulator is fed with power profiles of the trains while the interaction of the train and the system is included by means of a squeeze control implementation. The reversible substation works first in constant voltage mode but when the maximum power is encountered, the voltage is increased to operate in a constant power mode. The authors study how the no-load voltage, the control of the virtual resistance and the size of the inverters affect the efficiency and costs of the system. A similar procedure is proposed in [32] where a substation in forward mode is operated considering a two-segment approach, constant voltage segment and constant power segment. By means of this control the authors emulate a virtual impedance in both directions forward and reverse. Another novelty of this paper relates with the combination of transient and static solvers in the same platform. The steady state solver is used for performing energetic studies and also for initialising the transient solver when needed. The transient solver is able to provide remarks in the effect of the control parameters over the system along with the subsequent power quality issues.

As it can be observed from the previous paragraphs, many authors have proposed some mathematical models and solving algorithms for these kind of DC railways applications. These algorithms can be used for optimizing the planning stage and the operation of the railways. For instance, in [33] the authors propose a cooperative methodology in order to improve the overall efficiency of the system. There, a communication based train control (CBTC) is combined with distributed optimization procedures and a centralised train control (CTC). However, from all the cited works, only few papers focus in analyzing the impact and performance of the selected technology in a real case scenario. In this context, reference [34] is not focused in the simulation methodology itself, but rather in proposing a set of key operation indicators to evaluate the whole efficiency of DC railway systems. The performance indicators are divided in four categories: i) Power supply network, ii) Rolling Stock, iii) Depots and iv) Other supplementary infrastructure like the station lighting, escalators and tunnel ventilation. This previous paper highlights the need of accurate simulation tools suitable to assist designers with some key performance indicators under different scenarios to select those having the best efficiency. We fully agree with this statement and moreover consider as crucial to contribute with a detailed analysis of sufficient real case studies.

It is far beyond the scope of this paper to provide a complex description of the different mathematical models with their corresponding power flow algorithms. A detailed description of such models can be found in [13]. In this last reference the mathematical sustenance is described in detail and a set of simulations are presented to test the performance of the modelling and the algorithms in terms of accuracy, robustness, convergence and speed. However, in the aforementioned work, no detailed analyses of the single-instant cases were presented, being this the main purpose of this work, diverting attention from the mathematical part to focus on the evaluation of the results. To achieve this goal, the models presented in this paper are not general models in terms of their control feasibility but they represent the most extended real world applications.

The structure of this paper is as follows: Section 2 introduces the basic description of the presented models (network, devices and trains). The base case and its variations for building the different case studies is exposed in Section 3. In section 4, the authors describe single-instant cases in depth in order to evaluate all possible casuistic of the infrastructure and the trains. The analysis of these cases is useful to understand the different states of the system as it is explained in [35]. However, in these cases only specific time instants are analyzed and thus no conclusions can be extracted about the real effect of the devices and technologies over the system in a long time interval. This situation is overcome in Section 5 where the description and analysis of a realistic complex scenario is exposed for 8 possible variations, including aggregated simulation results attained for an 8-hour timeframe.

2 Network, devices and train models

This section provides a simplified yet accurate description of the different models. Regarding the network lines, a compact model has been adopted adding the negative feeder resistance to the positive one and considering the trains to be grounded. Such assumption is widely accepted by researchers [5, 6, 10, 13, 14]. The next subsections describe the train model considering an on-board accumulator, a substation model (with or without reversibility) and an off-board accumulator model.

2.1 Train plus on-board accumulator model

The mathematical model of the train plus the accumulator is represented in Fig. 1. The traction behaviour along the overcurrent and deep discharge curves (on the left part of the figure) can be seen in Fig. 1 a). The control philosophy implemented in this paper gives priority to the accumulation system. This means that the train power (P_{train}), which is the electrical power employed by the train to produce mechanical traction, will be provided by the accumulator if there is enough stored energy. The deep discharge protection curve determines: i) the value of the maximum power that the accumulator can provide depending on its actual state of charge (SOC), ii) the protection curve parameters $SOC1$ and $SOC2$ and iii) the maximum charge/discharge power (P_{max}) of the accumulator. All the electrochemical conversion efficiency of the battery is represented by the (EF) parameter of the accumulator converter. It must be remarked that the overcurrent protection strangulates the power that the train can extract from the catenary and the accumulator according to the overcurrent protection curve defined in turn by the parameters $V1$ and $V2$. The non-supplied power represents the difference between the mechanical power reference and the power that the train can consume when the overcurrent protection is activated.

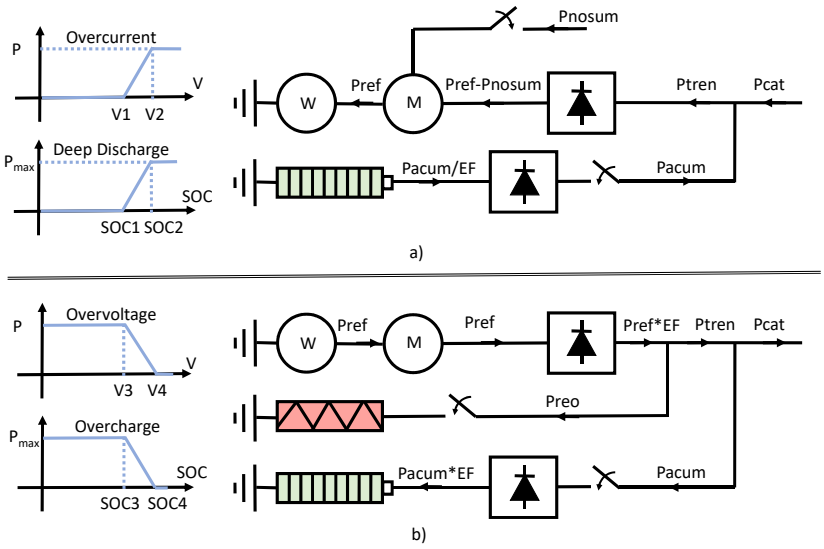

Fig. 1: Simplified train model representation. a) Train in traction mode. b) Train in braking mode. W stands for the wheels set and M represents the traction motor system.

In the same manner, the behaviour of the train in breaking mode (Fig. 1 b)) could be explained, but in this case we should consider the overvoltage curve of the train (also called squeeze control) that prevents power injection into the catenary when the voltage is too high. If the power can not be injected into the catenary or the accumulator, the train control derives part of the power to the rheostatic system.

2.2 Substation model with/without reversibility

Usually, reversible substations are equipped with a non-controlled diode rectifier plus a controlled IGBT based converter (see Fig. 2). The rectifier arrangement is usually oversized and it is used to inject power from the AC side into the DC system. This is represented by the forward resistance (Rf) characteristic represented in Fig. 2. When the substation is inversely polarised beyond a predefined parameter (Vr), the reverse IGBT branch is activated and the substation behaves as a resistance (Rr) injecting reverse power into the AC system. In the case of a unidirectional substation, the reverse resistance (Rr) is set to "infinite".

2.3 Off-board accumulator model

In Fig. 3, the accumulator model behavior is represented. As it can be observed, there is a deadband defined by the regulation voltage parameter ($Vreg$) and the parameter $dV2$. If the catenary voltage is within the mentioned deadband, the accumulator is not active. If the voltage increases beyond $V3$, the accumulator activates the charging mode and the charging power increases linearly until $V4$. On the contrary, if the catenary power is lower than $V2$, the accumulator control activates the discharging mode and the discharging power increases linearly while the catenary voltage decreases until voltage $V1$. Voltages $V1$, $V2$, $V3$ and $V4$ can be calculated using the regulation voltage ($Vreg$) and parameters $dV1$, $dV2$ and $dV3$. As in the on-board accumulator model, the off-board accumulator has also overcharging and deep discharge protections. The electrochemical conversion efficiency is represented by a parameter (EF) assigned to the off-board accumulator converter.

3 Base case and cases studies for instantaneous analysis

The base scenario is represented in Fig. 4. As it can be observed, for didactic purposes we have chosen a simple 750V (DC) linear system having a total length of 6km and three substations (S1, S2 and S3); placed at the initial, middle and end points respectively. All substations in this base scenario are non-reversible as it is represented in the current vs. voltage characteristic depicted on the top of Fig. 4. From this characteristic it can be inferred that the current can only flow from the AC side (represented using an equivalent DC system) [7, 12, 13] to the DC traction network. The resistance of all substations in forward mode (power flowing from AC to DC and negative current) has been set to

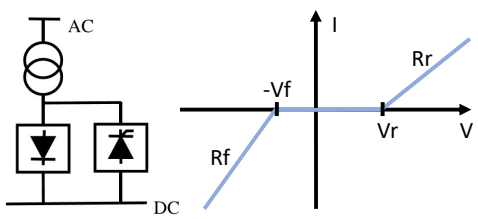

Fig. 2: Simplified substation model representation.

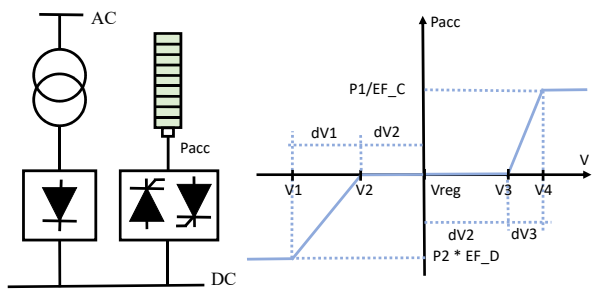

Fig. 3: Simplified off-board accumulator model representation.

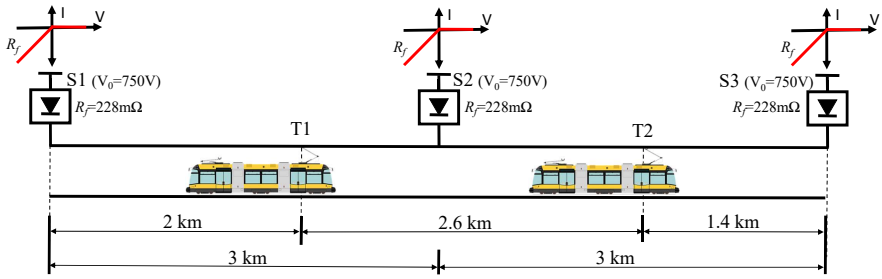

Fig. 4: Representation of the base system under study.

Table 1 Description of the cases and summary of the results in terms of total power provided by the system, burned power in the train rheostats, non-supplied power and overall efficiency of the system.

Cases	Substations type	On-board Accumulation	Train controls	P_{ref} Train 1 (kW)	P_{ref} Train 2 (kW)	Total P(kW)	Burned Power (kW)	Non-supp. Power (kW)	Eff. (%)
Case 1	Non-reversible	No	No	650	350	1335	0	0	74
Case 2	Non-reversible	No	No	-650	564	658	0	0	85
Case 3	Non-reversible	No	Yes	650	350	1144	0	209	78
Case 4	Non-reversible	No	Yes	-650	474	616	12	0	85
Case 5	Reversible	No	Yes	650	350	1144	0	209	78
Case 6	Reversible	No	Yes	-650	474	693	0	0	90
Case 7	Non-rev + Acc.	No	Yes	650	350	1280	0	0	90
Case 8	Non-rev + Acc.	No	Yes	-650	474	771	0	0	93
Case 9	Non-reversible	Yes	Yes	650	350	1197	0	0	93
Case 10	Non-reversible	Yes	Yes	-650	474	878	0	0	98

R_f=228 mΩ. This resistance represents the voltage drop and the losses equivalent to a set of power transformer plus rectifier. The rated power of each substation is P_r=0.35MW while the power transformer short circuit voltage is V_{cc}=8%. The resistances of the positive and negative feeders have been set to R_p=51mΩ/km and R_n=14mΩ/km respectively. Two trains (T1 and T2) are located at 2km and 4.6km from the initial point requiring maximum power demand and available for regenerating 0,65MW. All the efficiencies (electromechanical conversion of the train and the on-board/off-board accumulators) are set to 0.9 for the sake of simplicity. For a single-instant scenario, the exact state of charge is not relevant. However, the accumulators are not considered to be empty when they operate in discharge mode. Similarly, they are neither assumed to be full when they are in charge mode. In all cases the SOC is between SOC2 and SOC3 (see Fig. 1).

This condition will be labelled as the base scenario and it will be used for cases 1 and 2. In these two cases the train model is assumed as ideal and thus able to inject or consume all the reference power while no efficiency or protection curves are considered. The rest of the cases include variations with respect to this base scenario adding controls and different reversibility configurations for the substations and off-board/on-board accumulation systems. Table 1 summarises the different cases. Column 2 represents the type of substation, this is non-controlled diode based non-reversible substation (Non-reversible) or controlled IGBT based reversible substation (Reversible). The label (Non-rev + Acc.) is used for those substations that are non-reversible but are equipped with an off-board accumulation system for voltage support. Column 3 specifies whether or not the trains are equipped with on-board accumulation. It can be noticed that no cases with off-board accumulation at substation level and on-board accumulation were consider simultaneously as this situation is not realistic. Similarly, the concurrent use of reversible substations and off-board accumulation at substation level are not included as this combination can not be found in real world applications. Usually the off-board accumulation technology substitutes the reversibility feature of the substations. Column 4 details whether or not the trains have activated the overcurrent and overvoltage protection. As it can be observed, only in cases 1 and 2 (corresponding to the base scenario) these protection devices are deactivated. The 10-case set described in the table does not cover all possible combinations, but the most common an representative situations are exhibited. It must be pointed out that there is no case in which both trains are braking at the same time, in such situation, and with the quasi-steady approach adopted in this study, all the substations would be blocked and all regenerated power would be burned in the rheostatic system.

A summary of the results obtained in terms total power provided by the AC side to the DC traction system (column 7), burned power in the rheostatic apparatus of the trains (column 8), non-supplied power to the trains due to the overcurrent protection activation (column 9) and overall efficiency of the system (column 10) are also provided in Table 1. These results will be analysed in detail in the next section.

4 Casuistic Description Through Instantaneous Analysis

Fig. 5 contains the output information for all cases described in Table 1. The base scenario is represented in Fig. 4 a) and b) (cases 1 and 2 respectively). In case 1, the two trains are in traction model while in case 2 train T1 is braking. In both cases the overcurrent and overvoltage protection of the trains is deactivated.

4.1 Case 1 analysis

This case is intended to explain the information provided in each graph depicted in Fig. 5. Each case has three elements: i) the horizontal bar plot (on the top of each graph), ii) the network diagram with the trains and the power flowing through the lines and the rest of the devices (in the middle) and iii) the voltage profile along the catenary at the bottom. The horizontal bar plots have two bars, in the upper bar all the power provided to the system is represented. In case 1, all the power is provided by the AC system since both trains are accelerating and there is no storage elements. The total power provided to the system is 1335kW including the losses at the substations. As it can be observed, substation S1 is providing 418kW (upper bar of the horizontal bar plot), but only 347kW reach

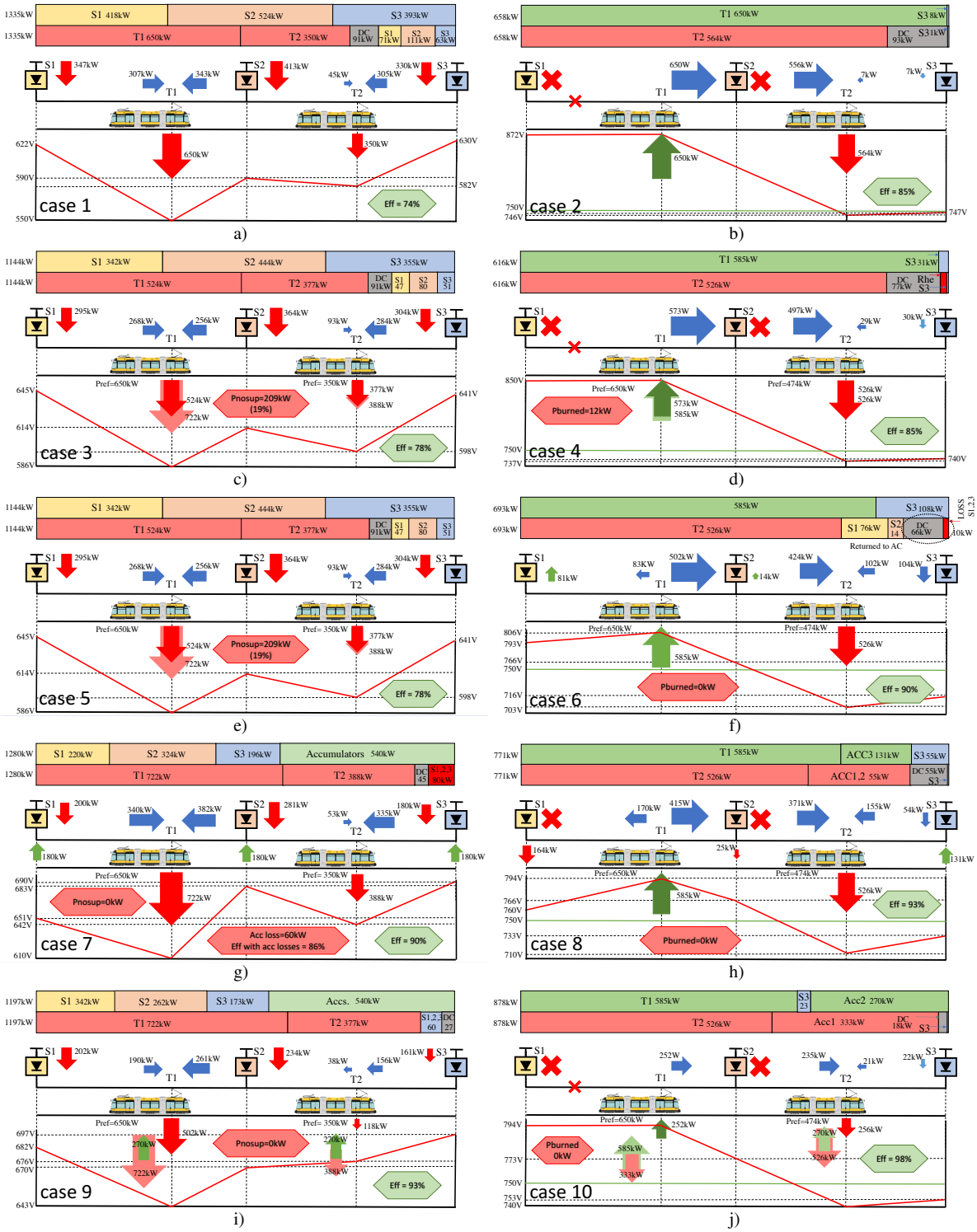

Fig. 5: Graphical representation of the 10 cases under study.

the DC traction systems (see the red arrow next to the S1 in the network diagram). The substation S1 losses (71kW) are represented in the lower bar of the horizontal bar plot that contains all the system consumption types including the losses. The sum of the power injections in the upper bar is always equal to the sum of the power consumption plus the losses represented in the lower bar. In this first case, trains T1 and T2 are demanding 650kW and 350kW respectively. As it was mentioned, all the power is provided by the substations, hence the losses at substations S1, S2 and S3 (71kW, 111kW and 63kW) and in the DC system are quite high (91kW). The voltage profile in this case is extremely low, falling to 550V and 582V in trains T1 and T2 respectively. The overall efficiency of the

system (without considering the internal efficiency of the trains) is 74%.

4.2 Case 2 analysis

In case 2 train T1 is braking and the voltage at substations S1 and S2 is higher than 750V, hence both of them are blocked. All the power injected by train T1 is employed to feed train T2. The distance between both trains is 2.6km, thus the losses in the DC system are significant and even higher than in the previous case (93kW). However, in the current scenario there are no losses in substations S1 and S2 since they are blocked and the power provided by substation S3 is very small (8kW) and the losses in this substation are neglectable (1kW). The sum of all power injected into the system in this case is nearly half of the power injected in case 1 and the efficiency is much higher (85%). The lower voltage in the system is present at train T2 and it is only 3V lower than the rated voltage even when the train is demanding 564kW from the catenary.

4.3 Case 3 analysis

In this and successive cases, trains are no longer ideal. The efficiency of the electromechanical conversion has been set to EF=0.9 and the overcurrent and overvoltage protections are activated. The voltages defining the overcurrent protection curve have be defined as $V1$=550V and $V2$=600V. Similarly, for the overvoltage protection curve, the voltages have been set to $V3$=850V and $V4$=900V. Case 3 is similar to Case 1 but with no-ideal trains. The power reference of trains T1 and T2 is 650kW and 350kW correspondingly, but due to the efficiency of the power conversion inside the train they demand from the catenary 722kW and 388kW. The voltage profile is too low and the overcurrent protection of both trains is activated reducing the available power that the trains can extract from the system. Train T1 can only extract 524kW and train T2 377kW, thus a total power of 209kW is not supplied and the acceleration rate of the trains in this instant would not fulfill the requirements. Even though the overall efficiency of the system is a little bit higher than in case 1, this is not a desirable situation.

4.4 Case 4 analysis

Case 4 is like case 2 but now a realistic model of the trains with efficiency lower than one and overcurrent-overvoltage protection is used. The parameters of the trains are the same as in case 3. Similarly to case 2, the overvoltage protection is activated as the voltage at train T1 is slightly higher than 850V. The mechanical power at train T1 in braking mode is 650kW. Due to the electromechanical conversion efficiency, the train can regenerate only 585kW. 12kW are derived to the rheostatic system due to the overvoltage protection and thus only 573kW are injected into the catenary. Again, the overall efficiency of the system is similar to the one attained in case 2 but this is not a desirable situation since as we are burning part of the regenerated power. The situation could be much worse if the power demanded by the train T2 decreases.

4.5 Case 5 analysis

Case 5 is similar to case 3 but now the substations are reversible, the reverse resistance is (Rr) is equal to the forward resistance (Rf) and the parameter Vr has been set to zero. Since both trains are in traction mode, the reversibility of the substations has no effect and the results obtained for this case are exactly the same as those in case 3 as expected.

4.6 Case 6 analysis

Case 6 is like case 4 but with reversible substations. The power injected by train T1 is used for feeding train T2 and delivering power back into the AC system through substations S1 and S2. The losses in the DC system are quite low. The aggregated losses in all substation is 10kW and there is no burned power since their reversibility help the system to alleviate the voltage increase provoked by the power injection from train T1. As a result, the overall efficiency of the system increases a 5% compared to case 4.

4.7 Case 7 analysis

Here the conditions are as in case 3 but now all substations are equipped with an off-board accumulator with a maximum charge/discharge power of P_{max}=200kW and a capacity of E_{max}=50kWh. The efficiency of the electrochemical conversion has been set to 90% and a state of charge SOC=50% has been assumed. The regulation voltage in this case is V_{reg}=750V while the parameters of the control curve $dV1$, $dV2$ and $dV3$ are fixed to 10V. Additionally, the parameters of the deep discharge and overcharge protection are $SOC1$=5%, $SOC2$=10%, $SOC3$=90% and $SOC4$=95%. In this case, all accumulators are providing the maximum power (180kW considering the conversion efficiency) and the overall efficiency of the system is 90%. This value drops to 86% when the efficiency of the accumulators is considered but still, this value is quite high when compared with the one attained in case 3. The most remarkable aspect to highlight in this case is the fact that all the power requested by the trains can be supplied as the voltage profile is higher given the voltage support function of the off-board accumulators. As it is depicted in the horizontal bar plot, nearly half of the power of the system is provided by the accumulators.

4.8 Case 8 analysis

The scenario described in case 4 has been here updated installing off-board accumulators in all substations with the same set up described in case 7. Again, the situation is improved substantially compared to case 4. The voltage profile in the whole system is now within the limits and the overvoltage protection of train T1 is not activated and there is no burned power. Substations S1 and S2 are blocked but the accumulators of these substations are charging at a rate of 164kW and 25kW respectively. The losses in the DC system are reduced and the losses at substation S3 (the one that is conducting) are nearly negligible. The overall efficiency of the system increases up to 93%.

4.9 Case 9 analysis

Finally, off-board accumulation is replaced by on-board accumulation. Case 9 is similar to case 3 but both trains are now equipped with on-board accumulation systems. In this case, the maximum charging and discharging power of the accumulators is P_{max}=300kW with an efficiency of EF=0.9. The capacity of the accumulators is E_{max}=10kWh and the parameters defining the deep discharge and overcharging protection are the same as the ones defined for the off-board accumulators. Both accumulators are being discharged at their maximum rate, but considering the efficiency, only 270kW are injected into the trains. Considering train T1, the mechanical power reference is 650kW, thus requesting 722kW (electrical power) while the net power demanded from the catenary is 502kW since the accumulator provides the rest of the power. In the case of train T2, the net demanded power is 118kW. In both trains the non-supplied power is 0kW and the power provided by the substations is around half of the power injected in the whole system. As it was expected, the losses in the DC system are very low (27kW) and the overall efficiency reaches 93%.

4.10 Case 10 analysis

Case 10 is like case 4 but the trains now include the same accumulators described in case 9. The efficiency in this case is the highest (98%). Train T1 is braking with a 650kW mechanical power reference. Considering the electromechanical efficiency, the train regenerates 585kW, 333kW are used for charging the on-board accumulator and 252kW are injected into the catenary. Train T2 is demanding a mechanical power of 474kW, so it needs 526kW. 270kW are provided by the accumulator and only 256kW are demanded from the catenary. Most of this power comes from train

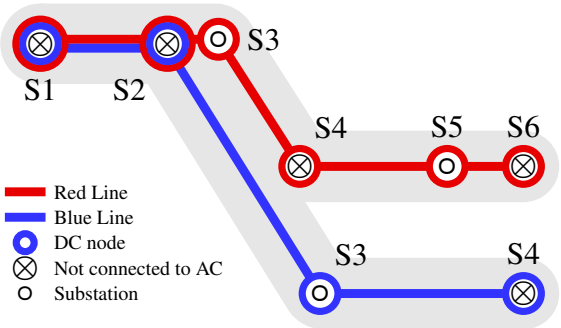

Fig. 6: Schematic representation of the case study

Table 2 Length of the different line segments in km

	S1 to S2	S2 to S3	S3 to S4	S4 to S5	S5 to S6
Red Line	4.316	0.500	13.800	7.848	4.378
Blue Line	4.316	25.284	7.335	-	-

Table 3 Summary of the train behaviour in the different trips, all data are in kWh

Trip	Required Mechanic. Energy	Mechanic. Regen. Capacity	Required Electrical Energy	Electrical Regen. Capacity	Min. Elect. Consump. Theoretical
S1 to S6 Red	245	112	258	106	151
S6 to S1 Red	240	107	253	102	151
S1 to S4 Blue	243	61	256	58	198
S4 to S1 Blue	187	99	197	94	103
Average Trip	229	95	241	90	151

T1 and only 22kW are provided by substation S3 since substations S1 and S2 are blocked. The losses in the DC system are just 18kW and the losses in substation S3 are neglectable. Off course, there is no burned power into the rheostatic braking system of the trains.

5 Real Complex Scenario Description and Analysis

In this section, we will analyze in depth the effect of the on board accumulation system over the trains and the network in different realistic scenarios. This section contains four subsections. In the first one, the basic feeding infrastructure (in lines and substations) is described. In the second subsection we will describe the trains. The third subsection is focused on describing the different scenarios that are later analyzed in subsection four.

5.1 Feeding Infrastructure

The case study in this section will focus on the study of a real network consisting of two lines of $30.84km$ and $36.93km$. The voltage level of the system is $3000V$. The simplified diagram of the network is depicted in Fig 6. The blue railway line is the longest. It has 9 stops and 4 electrical nodes labeled as S1, S2, S3 and S4. The red line shares the first two electrical nodes with the blue line and it has 17 stops and 6 electrical nodes labeled as S1, S2, S3, S4, S5 and S6. Hence, there are a total of 8 electrical nodes and 7 lines segments. Among the 8 nodes, only 3 of them represent feeding substations, the rest are nodes without any connection with the AC system. The three substations are placed in nodes S3 and S5 of the red line and in node S3 of the blue line. This substations have the same individual characteristics. All of them are composed by a power transformer with rated power of $3MW$ and a short circuit voltage of 5%. The no-load output voltage of the rectifier is $3000V$ and the voltage at rated load (1000A) is $2880V$. The equivalent impedance in each of the three substations in forward mode is $270m\Omega$. In the cases in which the substations are equipped with an IGBT controlled converter for reversibility, the equivalent impedance is double $540m\Omega$. The equivalent impedance of the overhead conductor and the rails (return circuit) are respectively $28.605m\Omega/km$ and $7m\Omega/km$. In Table 2 the lengths of the different segments of the red and blue lines can be observed. In the cases where the off-board accumulators are activated at substation level, each accumulator will have a maximum energy capacity of 25kWh and a maximum charge and discharge power of 1MW. Parameters V1, V2, V3 and V4 are set respectively to 2685V, 2985V, 3015V and 3315V while parameters SOC1,2,3 and 4 are 0%, 10%, 90% and 100%. The efficiency of the charging and discharging process is assumed in 95%. In all the simulations we will consider as 0% the initial state of charge of the off-board accumulation system.

5.2 Rolling Stock

The train used in both lines is an electrical multiple unit (EMU). The whole unit is 2.940m wide, 4.265m high and has a total length of 98.05m with an unladen weight of 157.3t. The units are composed of 5 cars, the two ends have a driver's cabin and normal floor. The middle car has a normal floor while the other two cars have a low floor. The 5 cars are supported on two types of bogies, the trailer bogie and the tractor. The tractor bogie is always shared between two cars. The train is designed to use a standard Iberian track gauge (1668mm) at a maximum speed of 120km/h with almost 1000 passengers, although it can reach 160km/h with minor modifications. The maximum total power of the train is 2.2MW and it has regenerative braking. In the base case, the trains are not equipped with on-board energy storage systems. However, the possibility of adding an on-board accumulator system based on ultracapacitors technology is considered. The electromechanical efficiency of the trains in traction and braking modes, as well as the electrochemical efficiency of the storage system in charging and discharging modes have been set to 0.95. The total accumulation system capacity is $7kWh$ and the rated charging and discharging power of the on-board energy storage device is 1MW.

Regarding the protection curves of the trains and the storage elements, the minimum and the regulation voltage of the train in traction mode ($V1, V2$) have been set to 1980V and 2280V. This same values have been selected for the minimum and regulation voltage of the energy storage system. In braking mode, the regulation voltage and the maximum voltage of the squeeze control ($V3, V4$) are set to 3300V and 3600V. In the cases in which the on-board accumulation system is activated, the system will be initialized with no charge.

Table 3 collects the data summarizing the behaviour of the trains in the different trips. The required mechanical power to complete the trip can be observed in the first column. It can be seen that the rails slope of the blue line is steeper because the difference between the power required for outward and return journeys is greater than in the red line. The average trip considering the two lines and both directions needs 229kWh. The mechanical regeneration capacity in column two refers to the available mechanical power able to be regenerated. Columns three and four contain the required electrical power and the electrical regeneration capacity considering already the efficiency of the electromechanical conversion. The electrical regeneration capacity is usually around 40% of the required electrical power, except in the S1 to S4 trip of the blue line. In this last case, as the train ascends a steep slope the regeneration capacity is much lower, around 22% of the required electrical power. The fifth column details the minimum electric consumption which is calculated subtracting the electrical regeneration capacity from the required electrical power. Off course this is a theoretical consumption which assumes that all electrical power is available for regeneration. This is not true for two main reasons. First, part of the power that is available to be injected in the catenary is burned in the rheostatic braking system when the squeeze control is activated to maintain the catenary voltage below the maximum level. In addition, if the train is equipped with on-board accumulation, the efficiency of the electrochemical conversion during the charging and discharging process also reduces the percentage of available regenerated power that can be reused. For these reasons, we will use these minimum consumption figures as a theoretical ceiling to compare the different

Table 4 Summary of the different proposed scenarios

Scenario Code	Traffic Density	Revers. Subst. System	Off-board Acc.	On-board Acc.	Number of Trains	Train Headway (min)
L1	Light	No	No	No	40	50
L2	Light	Yes	No	No	40	50
L3	Light	No	Yes	No	40	50
L4	Light	No	No	Yes	40	50
H1	Heavy	No	No	No	96	20
H2	Heavy	Yes	No	No	96	20
H3	Heavy	No	Yes	No	96	20
H4	Heavy	No	No	Yes	96	20

solutions, but we must be aware of the fact that we will not reach this theoretical ceiling.

5.3 Description of the Selected Scenarios

Eight different scenarios have been designed to study the influence of the accumulation system over the network as Table 4 details. There are 4 different paths for the trains, from S1 to S6 and from S6 to S1 in the red line and from S1 to S4 and S4 to S1 in the blue line. Two different traffic densities are considered. Light traffic scenarios use a train headway of 50 minutes with 10 departures for each of the above-described routes. Heavy traffic scenario launch 24 trains per route with a 20 minutes headway. The simulation interval is very similar for all scenarios and it goes from 8 hours and 18 minutes for the light traffic scenario to 8 hours and 28 minutes for the heavy traffic case. Each of the two traffic densities has been simulated without and within on-board accumulation, off-board accumulation and reversible substations. In all the cases, the basic feeding infrastructure without any modification is kept. The obtained results are presented in the next section it is also commented the effect of the on-board accumulation systems over the railway traction networks depending on the density of the traffic.

5.4 Results Analysis

The results obtained with the above-described scenarios are presented in this subsection. Fig. 7 represents a Marey diagram of the trains travelling through the red line. The horizontal axes represent time and the vertical ones represent the distance. Solid lines represent the trains moving from S1 to S6 while dash-dotted lines the train moving from S6 to S1. The vertical red lines represent the instants in which all substations are blocked at the same time. In the diagrams, only the first 80 minutes of simulation are represented, but in the top left corner we have added the information about the percentage of instants where all the substations are blocked for the whole simulation. As it will be demonstrated, this index represents a very good indicator of the electrical congestion of the network. In cases L2 and H2, the use of reversible substations obviously remove completely the cases in which all substations are blocked. The percentage of blocked cases in scenarios with on-board and of-board accumulation is similar. From this point of view, both solutions are equivalent. The blocked cases in both scenarios with non-reversible substations without any kind of accumulation are quite high. However, it should be remarked that when the train headway is decreased from 50min to 20min, the percentage of blocked instants drops to 2%.

In order to evaluate the effect of the four proposed approaches (conventional non-reversible substations, reversible substations, non-reversible substations with off-board energy storage and non-reversible substations with on-board energy storage), aggregated values of all representative energies in the system are obtained for the whole simulation time interval (around 8 hours). The results are presented in three different tables. Table 5 exhibits the amount of global energy used in different parts of the system expressed in MWh. There it can also be seen the total energy consumed by the trains or the total energy burned in their rheostatic braking system. This table will be commented in detail in the next paragraphs. Table 6 includes the energy balance in different parts of the system referred to the total electrical energy required by the trains. Finally, Table 7 contains the different energies averaged by the number of trains. The three tables may be redundant but the authors strongly believe that it is worth to include them all to provide the reader with sufficient understanding.

The total energy required by the trains in the system is represented in the first row of the Table 5. It depends on the train headway, as well on the regeneration capacity and the minimum consumption represented in rows 2 and 3 respectively. The minimum consumption is calculated considering that all the regenerated energy can be reused by the trains. The regeneration capacity represent a 37% of the power required by the trains, hence the minimum consumption is around 62% (151kWh per train). The energy required by the trains varies in a linear way depending on the number of trains, being 9.66MWh in the scenario with 40 trains and 23.08MWh in the 96-train scenario. The fourth row in Tables 5 and 6, and the first row in Table 7 represent the real energy consumed by the trains. As it can be observed, this energy is equal to the required energy in the second scenario in which the system is equipped with reversible substations. In the rest of the scenarios, this energy is a little bit lower. In some cases, when all substations are blocked, some of the units that are in traction mode can not absorb the requested power. The average requested power per train and per trip is 241kWh (see Table 3).

Table 5 Summary of the trains and the network behaviour in the different scenarios

	Energy (MWh)							
Scenario	L1	L2	L3	L4	H1	H2	H3	H4
Req. Electrical	9.66	9.66	9.66	9.66	23.08	23.08	23.08	23.08
Reg. Capacity	3.62	3.62	3.62	3.62	8.65	8.65	8.65	8.65
Min. Consumpt.	6.04	6.04	6.04	6.04	14.43	14.43	14.43	14.43
Train. Demand	8.94	9.66	9.59	7.30	21.67	23.08	22.94	17.52
Train Inject.	1.61	3.62	3.26	0.58	5.93	8.65	8.26	2.00
Train Net	7.32	6.04	6.32	6.73	15.74	14.43	14.68	15.52
Rheostatic	2.01	0.00	0.36	0.49	2.72	0.00	0.39	0.79
Non Supp	0.72	0.00	0.07	0.20	1.41	0.00	0.14	0.43
Prov. Subs.	7.64	8.03	6.84	6.93	16.53	17.31	15.62	16.01
Inject. Subs.	0.0	1.69	0.0	0.0	0.0	2.13	0.00	0.0
Sub. Net	7.62	6.34	6.84	6.91	16.52	15.18	15.62	16.01
Grid Losses	0.29	0.30	0.52	0.18	0.78	0.75	0.95	0.48

Table 6 Summary of the trains and the network in the different scenarios (%)

Energy in % respecT to the electrical energy required by trains								
	L1	L2	L3	L4	H1	H2	H3	H4
Req. Electrical	100	100	100	100	100	100	100	100
Reg. Capacity	37	37	37	37	37	37	37	37
Min. Consumpt.	62	62	62	62	62	62	62	62
Train Demand	92.5	100	99.2	75.5	93.9	100	99.3	75.9
Train Inject.	16.6	37	33.7	5.9	25.7	37.4	35.8	8.6
Train Net	75.8	62.4	65.4	69.6	68.2	62.5	63.5	67.2
Rheostatic	20.8	0	3.7	5.0	11.7	0	1.6	3.4
Non Supp	7.5	0	0.7	2.0	6.0	0	0.6	1.8
Prov. Subs.	79.1	83.0	70.8	71.7	71.6	75.0	67.7	69.3
Inject. Subs.	0	17.4	0	0.1	0	9.2	0	0
Sub. Net	78.8	65.6	70.8	71.5	71.5	65.7	67.6	69.3
Grid Losses	3.0	3.1	5.3	1.9	3.3	3.2	4.1	2.0

Table 7 Averaged contribution per train

	Energy (kWh)							
	L1	L2	L3	L4	H1	H2	H3	H4
Train Demand	224	241	240	183	226	241	239	183
Train Inject.	40	91	82	15	62	90	86	21
Train Net	183	151	158	168	164	150	153	162
Rheostatic	50	0	9	76	28	0	4	69
Non Supp	18	0	2	4	15	0	1	3
Prov. Subs.	191	201	171	173	172	180	163	167
Inject. Subs.	0	42	0	0	0	22	0	0
Sub. Net	191	159	171	173	172	158	163	167
Grid Losses	7	8	13	5	8	8	10	5

In the conventional case with no reversible substations and no accumulation, the average train is only able to consume 224kWh in the light-traffic scenario and 226kWh in the heavy-traffic one. Off board accumulation improves the situation substantially since the average train is able to consume nearly 100% of the requested energy. In the cases having on-board energy storage, the average train consumes from the catenary 183kWh, only 76% of the required power. However, in this conditions, part of the energy is provided by the on-board energy storage system. The best indicator to verify if the trains are able to consume all the required power is the non supplied energy (row 8 in Tables 5 and 6 and row 5 in Table 7). As it can be observed, the non-supplied energy in the on-board energy storage cases is in the same order of magnitude, independently of the existence of on-board or off-board energy storage. In the cases with on-board accumulation, the non supplied energy is around 2% of the required power, while in the cases with off-board accumulation, the non-supplied energy drops to 0.7%.

It is also worth to recall the comparison between the regeneration capacity and the actual power injected by the trains in the DC traction network. Again, in the cases with reversible substations the trains are able to inject all the regenerated power (37% of the required). In conventional cases with no accumulation, this percentage drops substantially. In the light traffic scenario, the trains can inject only 16% of the required power. Nonetheless, the situation is improved in the heavy traffic scenario (25%). The cases with off-board accumulation are very close to the maximum with 33% and 35%. In the cases with on-board accumulation, trains only inject around 7% as in this cases part of the regenerated power is used to charge the internal accumulation system.

In the last rows of Tables 5, 6 and 7; we can observe the energy provided by the substations (Prov. Subs.), the energy returned to the AC grid (Inject. Subs), the net energy in the substations (Sub. Net) and the grid losses. Particularly, if we analyse in Table 7 the cases with reversible substations, it can be seen that the substations provide a net power close to 159kWh per train and per trip, only 8kWh above the minimum theoretical consumption. This difference represents the network losses. In the rest of the cases, the net energy provided by the substations is substantially higher, reaching 191kWh (40kWh above the minimum consumption in case L1). It also should be remarked that when comparing cases L2 and H2, the energy provided by the substations is higher when the train headway is bigger. This is an evidence on how increasing the train frequency sometimes benefits the use of the regenerated power within the DC traction network. Another important consideration is the economic benefit of giving back energy to the AC system. It is true that reversible substations are much better from the point of view of the stability of the system and the operation is also easier. However, the economic benefit that the train operator receives for returning back power to the AC system is nearly zero in most of the systems. In this regard for instance, we need to consider that in the light traffic scenario we have to pay for 201kWh per train; while on the other hand scenarios L3 and L4 require only 171 and 173kWh, thus the cost of the energy will 15% lower using the accumulation.

6 Conclusions

In the present paper a set of different case studies for railway power systems have been presented. A variety of technologies and configurations were included and the results have been analysed using the referred models embedded in a quasi-static power flow solver. Reversible substations were compared with conventional ones incorporating the use of on-board and off-board accumulation. First, ten different instantaneous cases were studied considering the most representative and common scenarios that can be encountered when feeding the trains and setting up the system. By means of this set of case studies, it was possible to determine the proper technological mix that came up with the best results. Then, 8 realistic complex scenarios were studied for long simulation intervals and the aggregated values of all energies in the system were attained

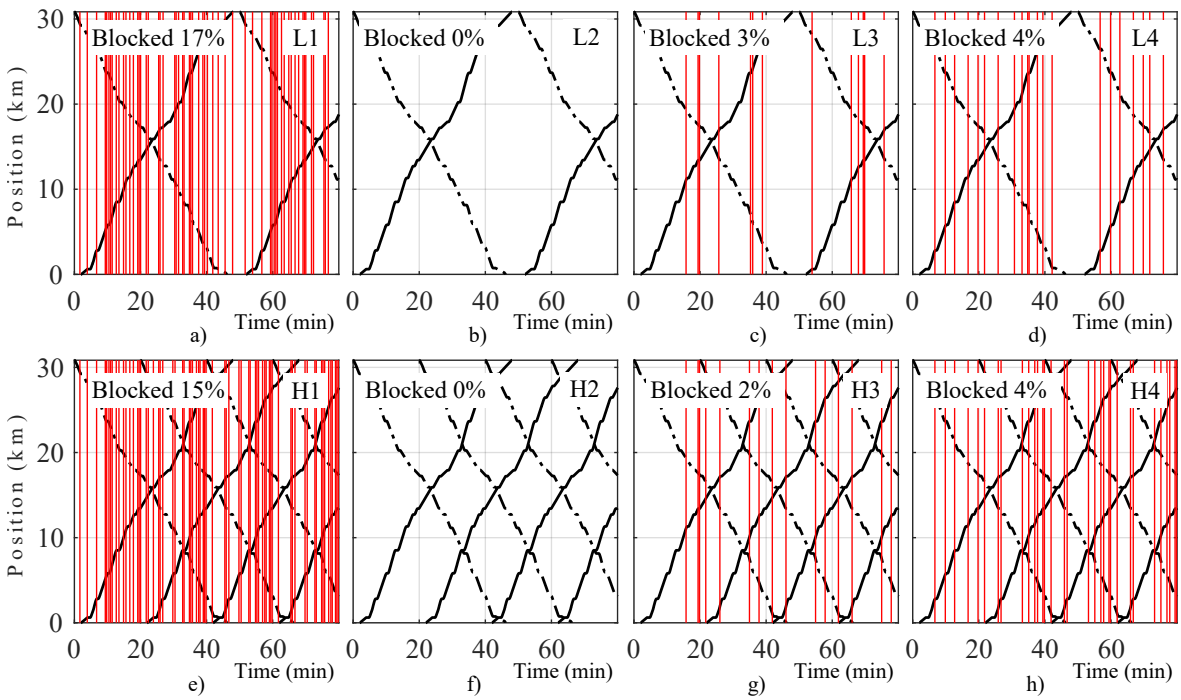

Fig. 7: Marey diagrams representing the first 80 minutes schedule of the red line in the different scenarios. Solid lines represent the trains moving from S1 to S6 while dash-dotted lines represent the trains moving from S6 to S1. The vertical red lines mark the instants in which all the substations in the system are blocked due to the high regenerated power surplus. The number in the top-left corner of each subfigure represents the percentage of instants in which all the substations are blocked at the same time for the whole simulation interval. The scenario is indicated in the top-right corner of each subfigure.

and analysed in order to measure the real impact of the different technologies over the system. The exposed models in combination with a power flow solver represent a highly useful instrument to better understand how the system configurations affect the overall efficiency. The development of these kind of simulation tools and models is critical for designing railway electrical systems in an optimal way.

Acknowledgment

The authors would like to thank to CAF Turnkey & Engineering, specially to Peru Bidaguren and Urtzi Armendariz for their support during the development of this research. We would like also to thank Xavier Dominguez for his valuable help during the revision process of this paper.

7 References

1 Langerudy, A.T., Mousavi, S.M.: 'Hybrid railway power quality conditioner for high-capacity traction substation with auto-tuned DC-link controller', *IET Electrical Systems in Transportation*, 2016, **6**, (3), pp. 207–214
2 Arboleya, P., Bidaguren, P., Armendariz, U.: 'Energy is on board: Energy storage and other alternatives in modern light railways', *Electrification Magazine, IEEE*, 2016, **4**, (3), pp. 30–41
3 Takagi, R., Amano, T.: 'Optimisation of reference state-of-charge curves for the feed-forward charge/discharge control of energy storage systems on-board DC electric railway vehicles', *IET Electrical Systems in Transportation*, 2015, **5**, (1), pp. 33–42
4 Li, Q., Wang, T., Dai, C., Chen, W., Ma, L.: 'Power management strategy based on adaptive droop control for a fuel cell-battery-supercapacitor hybrid tramway', *IEEE Transactions on Vehicular Technology*, 2018, **67**, (7), pp. 5658–5670
5 Aguado, J.A., Racero, A.J.S., de la Torre, S.: 'Optimal operation of electric railways with renewable energy and electric storage systems', *IEEE Transactions on Smart Grid*, 2018, **9**, (2), pp. 993–1001
6 Pilo, E., Mazumder, S.K., González.Franco, I.: 'Smart electrical infrastructure for AC-fed railways with neutral zones', *IEEE Transactions on Intelligent Transportation Systems*, 2015, **16**, (2), pp. 642–652
7 Mohamed, B., Arboleya, P., González.Morán, C.: 'Modified current injection method for power flow analysis in heavy-meshed DC railway networks with non-reversible substations', *IEEE Transactions on Vehicular Technology*, 2017, **66**, (9), pp. 7688–7696
8 Tian, Z., Hillmansen, S., Roberts, C., Weston, P., Zhao, N., Chen, L., et al.: 'Energy evaluation of the power network of a DC railway system with regenerating trains', *IET Electrical Systems in Transportation*, 2016, **6**, (2), pp. 41–49
9 de la Torre, S., Sánchez.Racero, A.J., Aguado, J.A., Reyes, M., Martínez, O.: 'Optimal sizing of energy storage for regenerative braking in electric railway systems', *IEEE Transactions on Power Systems*, 2015, **30**, (3), pp. 1492–1500
10 López.López, A.J., Pecharromán, R.R., Fernández.Cardador, A., Cucala, A.P.: 'Smart traffic-scenario compressor for the efficient electrical simulation of mass transit systems', *International Journal of Electrical Power & Energy Systems*, 2017, **88**, pp. 150 – 163
11 Khayyam, S., Berr, N., Razik, L., Fleck, M., Ponci, F., Monti, A.: 'Railway system energy management optimization demonstrated at offline and online case studies', *IEEE Transactions on Intelligent Transportation Systems*, 2018, **19**, (11), pp. 3570–3583
12 Jabr, R.A., Dzafic, I.: 'Solution of DC railway traction power flow systems including limited network receptivity', *IEEE Transactions on Power Systems*, 2017, **PP**, (99), pp. 1–1
13 Arboleya, P., Mohamed, B., El.Sayed, I.: 'DC railway simulation including controllable power electronic and energy storage devices', *IEEE Transactions on Power Systems*, 2018, **PP**, (99), pp. 1–1
14 Yang, Z., Yang, Z., Xia, H., Lin, F.: 'Brake voltage following control of supercapacitor-based energy storage systems in metro considering train operation state', *IEEE Transactions on Industrial Electronics*, 2018, **PP**, (99), pp. 1–1
15 Perin, I., Walker, G.R., Ledwich, G.: 'Load sharing and wayside battery storage for improving ac railway network performance, with generic model for capacity estimation, part 1', *IEEE Transactions on Industrial Electronics*, 2019, **66**, (3), pp. 1791–1798
16 Alfieri, L., Battistelli, L., Pagano, M.: 'Energy efficiency strategies for railway application: alternative solutions applied to a real case study', *IET Electrical Systems in Transportation*, 2018, **8**, (2), pp. 122–129
17 Kleftakis, V.A., Hatziargyriou, N.D.: 'Optimal Control of Reversible Substations and Wayside Storage Devices for Voltage Stabilization and Energy Savings in Metro Railway Networks', *IEEE Transactions on Transportation Electrification*, 2019, **5**, (2), pp. 515–523
18 Razik, L., Berr, N., Khayyamim, S., Ponci, F., Monti, A.: 'Rem-s–railway energy management in real rail operation', *IEEE Transactions on Vehicular Technology*, 2018, pp. 1–1
19 Alfieri, L., Battistelli, L., Pagano, M.: 'Impact on Railway Infrastructure of Wayside Energy Storage Systems for Regenerative Braking Management: a Case Study on a Real Italian Railway Infrastructure', *IET Electrical Systems in Transportation*, 2019,
20 Ceraolo, M., Giglioli, R., Lutzemberger, G., Bechini, A. 'Cost effective storage for energy saving in feeding systems of tramways'. In: Electric Vehicle Conference (IEVC), 2014 IEEE International. (, 2014. pp. 1–6
21 Roch.Dupré, D., Cucala, A.P., Pecharromán, R.R., López.López, Á.J., Fernández.Cardador, A.: 'Evaluation of the impact that the traffic model used in railway electrical simulation has on the assessment of the installation of a Reversible Substation', *International Journal of Electrical Power & Energy Systems*, , pp. 201–210
22 Clerici, A., Tironi, E., Castelli.Dezza, F.: 'Multiport Converters and ESS on 3-kV DC Railway Lines: Case Study for Braking Energy Savings', *IEEE Transactions on Industry Applications*, 2018, **54**, (3), pp. 2740–2750
23 Mayet, C., Horrein, L., Bouscayrol, A., Delarue, P., Verhille, J.N., Chattot, E., et al.: 'Comparison of different models and simulation approaches for the energetic study of a subway', *Vehicular Technology, IEEE Transactions on*, 2014, **63**, (2), pp. 556–565
24 Mayet, C., Delarue, P., Bouscayrol, A., Chattot, E., Verhille, J.N.: 'Comparison of different EMR-based models of traction power substations for energetic studies of subway lines', *Vehicular Technology, IEEE Transactions on*, 2016, **65**, (3), pp. 1021–1029
25 Mayet, C., Bouscayrol, A., Delarue, P., Chattot, E., Verhille, J.N.: 'Electrokinematical simulation for flexible energetic studies of railway systems', *IEEE Transactions on Industrial Electronics*, 2018, **65**, (4), pp. 3592–3600
26 Khodaparastan, M., Dutta, O., Saleh, M., Mohamed, A.A.: 'Modeling and Simulation of DC Electric Rail Transit Systems With Wayside Energy Storage', *IEEE Transactions on Vehicular Technology*, 2019, **68**, (3), pp. 2218–2228
27 Zhu, X., Hu, H., Tao, H., He, Z.: 'Stability Analysis of PV Plant-Tied MVDC Railway Electrification System', *IEEE Transactions on Transportation Electrification*, 2019, **5**, (1), pp. 311–323
28 Boudoudouh, S., Maaroufi, M.: 'Renewable Energy Sources Integration and Control in Railway Microgrid', *IEEE Transactions on Industry Applications*, 2019, **55**, (2), pp. 2045–2052
29 Sengor, I., Kilickiran, H.C., Akdemir, H., Kekezogcaronlu, B., Erdinc, O., Catalao, J.P.S.: 'Energy Management of a Smart Railway Station Considering Regenerative Braking and Stochastic Behaviour of ESS and PV Generation', *IEEE Transactions on Sustainable Energy*, 2018, **9**, (3), pp. 1041–1050
30 Tian, Z., Zhao, N., Hillmansen, S., Roberts, C., Dowens, T., Kerr, C.: 'SmartDrive: Traction Energy Optimization and Applications in Rail Systems', *IEEE Transactions on Intelligent Transportation Systems*, 2019, **20**, (7), pp. 2764–2773
31 Zhang, G., Tian, Z., Tricoli, P., Hillmansen, S., Wang, Y., Liu, Z.: 'Inverter Operating Characteristics Optimization for DC Traction Power Supply Systems', *IEEE Transactions on Vehicular Technology*, 2019, **68**, (4), pp. 3400–3410
32 Zhang, G., Tian, Z., Tricoli, P., Hillmansen, S., Liu, Z.: 'A new hybrid simulation integrating transient-state and steady-state models for the analysis of reversible DC traction power systems', *International Journal of Electrical Power and Energy Systems*, , pp. 9–19
33 Bai, Y., Cao, Y., Yu, Z., Ho, T.K., Roberts, C., Mao, B.: 'Cooperative Control of Metro Trains to Minimize Net Energy Consumption', *IEEE Transactions on Intelligent Transportation Systems*, 2019, pp. 1–15
34 Gonzï£¡lez.Gil, A., Palacin, R., Batty, P.: 'Optimal energy management of urban rail systems: Key performance indicators', *Energy Conversion and Management*, 2015, **90**, pp. 282–291
35 Mohamed, B., El.Sayed, I., Arboleya, P. 'DC railway infrastructure simulation including energy storage and controllable substations'. In: 2018 IEEE Vehicle Power and Propulsion Conference - VPPC. (, 2018. pp. 1–6